UV Curable Formulations for Deep UV LEDs

Haruyuki Okamura[a], Shoichi Niizeki[b], Tetsumi Ochi[b] and Akikazu Matsumoto[a]
[a]Department of Applied Chemistry, Osaka Prefecture University
1-1, Gakuen-cho, Naka-ku, Sakai, Osaka 599-8531, Japan
[b]Nikkiso Giken Co., Ltd.
498-1, Shizutani, Makinohara-shi, Shizuoka 421-0496, Japan

Introduction

UV curing materials have been extensively studied due to the wide applicability such as negative-type photoresists, coating materials and printing materials[1]. Recently, UV light-emitting diodes (UV LEDs) have attracted much attention as the light sources for UV-curing technologies due to their long life, high stability, bright output, compactness, and low power requirement. Among the UV LED technologies for photocuring, much interest is focused on near UV and/or visible LEDs due to their low cost and high light intensities. Much interest was focused on photoinitiators[2-7] and sensitizers[8] which are applicable to photocuring systems. On the other hand, there are a few reports on the application of deep UV LEDs for sensors[9,10] and UV LED encapsulant[11]. To the best of our knowledge, there are no comprehensive studies of the formulations for deep UV LEDs which are applicable to practical use.

In this work, we investigated the formulations of acrylates which were applicable to deep UV LED lamps. The mixtures of acrylate monomers and photoinitiators were irradiated by deep UV lamps which emit 265, 285, or 300-nm lights. The effect of photoinitiators, irradiation wavelength, and atmosphere on the conversion of the acryl unit was investigated using FT-IR spectroscopy and photoDSC measurements.

Experimental

Materials

Structures of chemicals used were shown in Fig. 1. Photoinitiators 1-hydroxy-1-cyclohexyl phenyl ketone (HCPK), 2-hydroxy-2-methyl-1-phenyl-propan-1-one (HMPP), 2,2-dimethoxy-2-phenylacetophenone (DMPA), and diphenyl(2,4,6-trimethylbenzoyl)phosphine oxide (TPO) were used as received. Photoinitiators *O*-benzoyl 2,3-butanedione monooxime (BAOBE) and *O*-acetyl 2,3-butanedione monooxime (BAOAE) were prepared as reported[12]. Multifunctional acrylates dipentaerythritol hexaacrylate (A-DPH) and pentaerythritol triacrylate (A-TMM-3LMN) were kindly donated by Shin-Nakamura Chemical Co., Ltd. and used without further purification.

Method

Commercially available deep UV LED lamps (SMD series: 265, 285, and 300 nm) from Nikkiso Giken (Shizuoka, Japan) were used as light sources. An array of 2 x 12 LED packages was placed on a board with a heat sink within the area of 3 cm x 10 cm rectangle in the light sources. Light intensities of the deep UV LEDs on irradiation at 265, 285, and 300 nm were 0.28, 0.74, and 0.70 mW/cm^2, respectively.

A mixture of multifunctional acrylates A-DPH or A-TMM-3LMN and photoinitiators was spin-coated on a silicon wafer and laminated by a CaF_2 plate if needed. Irradiation was performed using the deep UV LED lamps in air. Conversion of the acryl unit in the film was determined by FT-IR measurements using the peak at 1635 cm^{-1} ascribed to the acryl unit.

PhotoDSC studies were carried out as follows. A mixture of multifunctional acrylates and photoinitiators (ca. 2 mg) was placed in a 5-mm-diameter aluminum pan. Irradiation was performed using a Xenon lamp (Asahi Spectra, MAX-301, 300 W) through band-path filters at 254, 285, 300, or 365 nm combined with a mirror which passes the light below 400 nm using a Shimadzu UV-DSC system in air or under N_2.

Conversion of the acryl unit in the blended film was determined using the heat value of 20.6 kcal/mol for the reaction of the acrylate double bond[13].

Measurements

FT-IR measurements were carried out using a JASCO FT/IR-4600. UV-vis spectra were taken on a Shimadzu UV-2400 PC. The intensity of the light was measured with an Orc Light Measure UV-M02 or Ushio USR-45VA. Thickness of the films was determined by using a Nanometrics M3000 interferometer or a peacock dial thickness gauge (model G, OZAKI MFG.).

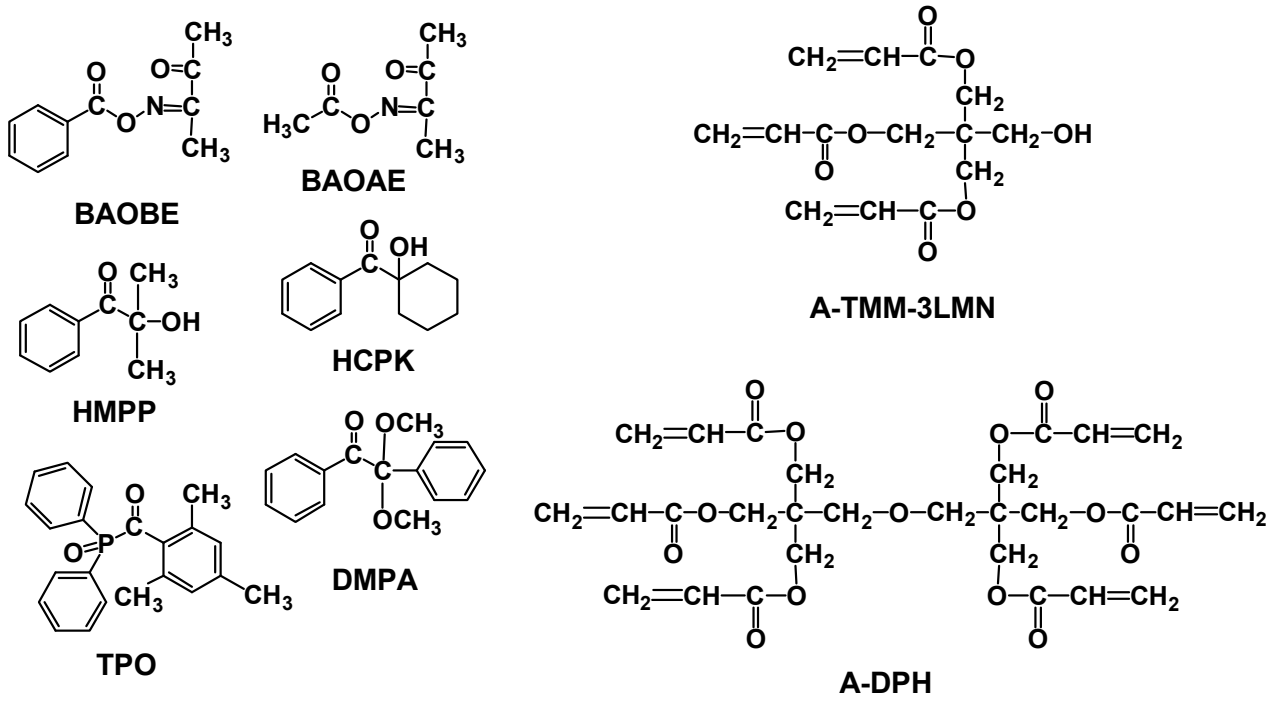

Fig. 1. Structures of chemicals used.

Results and discussion

Characteristics of photoinitiators and light sources

UV curing is generally achieved by photopolymerization which is obtained by the utilization of photoinitiators and photocrosslinking agents. Photoinitiators are key materials for UV-curing processes. The first stage in UV curing system is the absorption of a photon from the incident radiation by the photoinitiators. Light absorption by the photoinitiators requires that the emission line from the light source overlaps with an absorption band of the photoinitiators. Thus, the absorption spectrum of the photoinitiator must be carefully selected[14].

In this work, we selected six compounds of photoinitiators including *O*-benzoyl 2,3-butanedione monooxime (BAOBE)[12] which was found to be useful for 254-nm irradiation[15]. On irradiation, BAOBE is photolyzed to produce benzoyl radical and iminyl radical[16], which initiate radical polymerization in the system. The other photoinitiators are typically type I photoinitiators which are photolyzed to produce two radical species[14]. Figure 2 shows UV-vis spectra of the photoinitiators in acetonitrile. The molar absorption coefficient values were also summarized in Table 1.

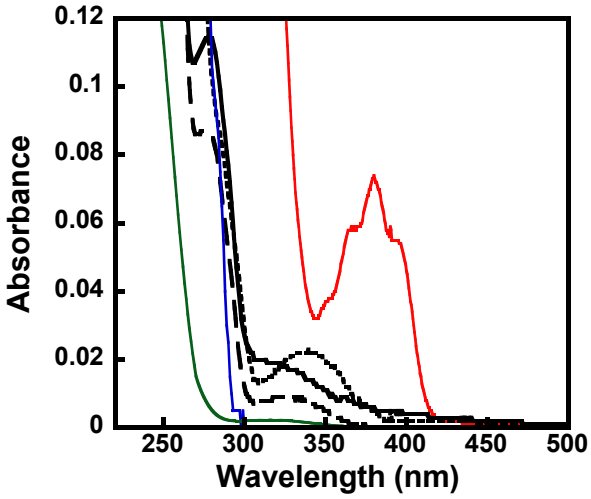

Fig. 2. UV-vis spectra of TPO (red line), DMPA (dotted line), HCPK (broken line), HMPP (solid line), BAOBE (blue line) and BAOAE (green line) in acetonitrile (1.0×10^{-4} M).

Table 1. Molar absorption coefficient values of TPO, DMPA, HCPK, HMPP, BAOBE, and BAOAE in acetonitrile.

wavelength (nm)	$\varepsilon \times 10^{-4}$					
	BAOBE	BAOAE	HMPP	HCPK	DMPA	TPO
254	0.700	0.068	0.644	0.629	0.883	0.679
265	0.235	0.036	0.119	0.110	0.432	0.466
285	0.075	0.003	0.099	0.072	0.086	0.376
300	0.000	0.002	0.027	0.012	0.029	0.393
365	0.000	0.000	0.008	0.001	0.011	0.058

In this work, we investigated deep UV LEDs at 265, 285, and 300 nm in addition to 365-nm light and medium pressure mercury lamp which has multiple line spectra as a conventional light source. The power spectra of the light sources are shown in Fig. 3. For photoDSC studies, a Xenon lamp was used instead of deep UV LEDs. The power spectra were also shown in Fig. 4.

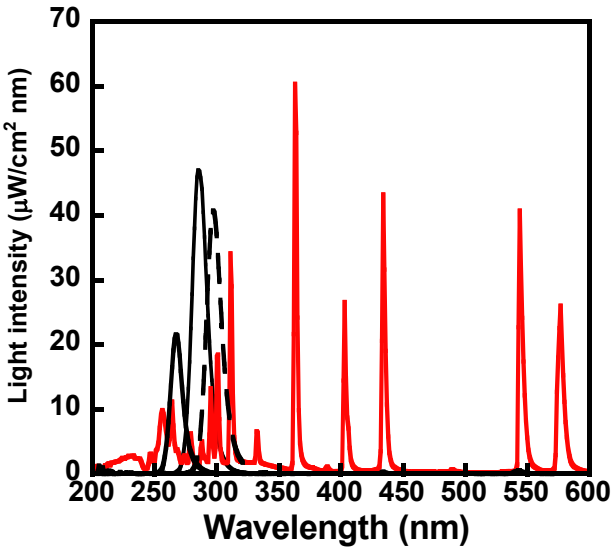

Fig. 3. Power spectra of deep-UV LEDs. Bold line: 265-nm light. Solid line: 285-nm light. Broken line: 300-nm light. For comparison, power spectrum of medium pressure mercury lamp (red line) was also shown.

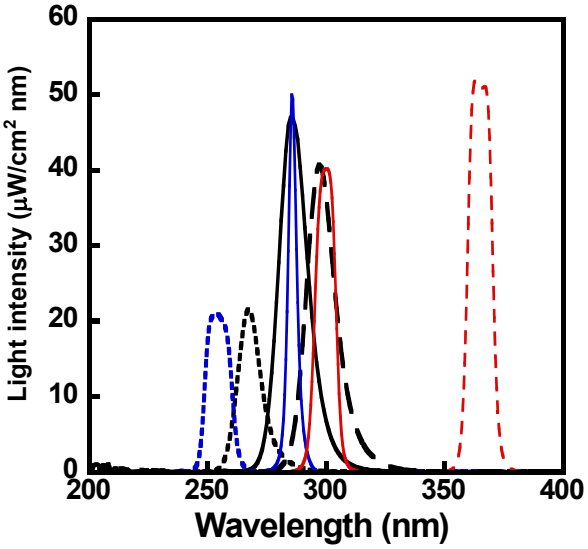

Fig. 4. Power spectra of light for photoDSC studies. Blue and dotted line: 254-nm light. Blue and solid line: 285-nm light. Red and solid line: 300-nm light. Red and broken line: 365-nm light. For comparison, power spectra of deep-UV LEDs were also shown. Bold line: 265-nm light. Solid line: 285-nm light. Broken line: 300-nm light.

Photocuring behavior

Photocuring was carried out using deep UV LEDs. The mixture of hexaacrylate A-DPH and photoinitiators was coated on a Si wafer. The thickness of the films was adjusted between 0.5 to 6 μm due to technical limitations. Conversion of acrylates in A-DPH was monitored using FT-IR spectroscopy. Figure 5 shows the FT-IR spectral changes of 0.7-μm-thick A-DPH/HCPK (1:0.005, wt/wt) blended film on irradiation at 285 nm in air. The conversions of acryl groups in the film were determined by the decrease of the peak at 1635 cm^{-1} in FT-IR spectra. After irradiation for 20 min, 20% decrease of the peak was observed.

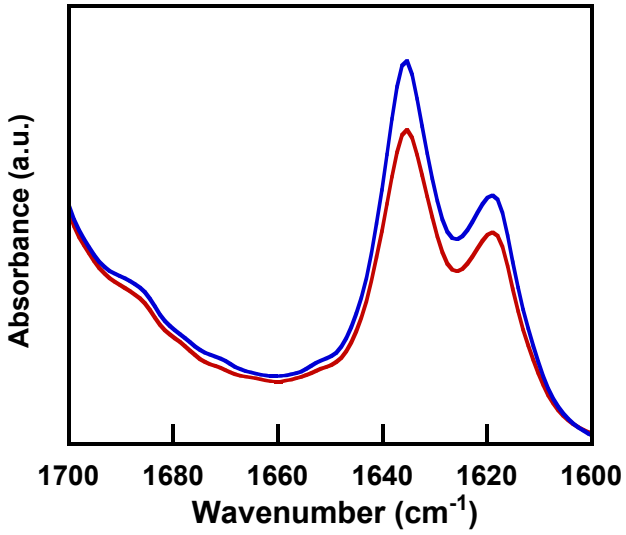

Fig. 5. FT-IR spectral changes of 0.7-μm-thick A-DPH/HCPK (1:0.005, wt/wt) blended film on irradiation at 285 nm in air. Blue line: before irradiation. Red line: after irradiation. Irradiation time: 20 min. Light intensity: 0.7 mW/cm^2.

The effect of irradiation dose and irradiation atmosphere on conversion was investigated using the formulation and film thickness. Figure 6 shows the effect of irradiation dose on the conversion of 0.7-μm-thick A-DPH/HCPK (1:0.005, wt/wt) blended film on irradiation at 285 nm in air and without air. The conversion proportionally increased with irradiation dose regardless of atmospheric conditions. The results indicate that there is low oxygen inhibition in the system. The observation strongly supported the recent report[17] that irradiation of deep UV light is effective to reduce oxygen inhibition.

The effect of photoradical initiators and irradiation wavelength on irradiation in air was investigated. Figure 7 shows the conversion rate of A-DPH with photoinitiators on irradiation at several wavelengths. In the experimental conditions, the irradiation lights completely penetrate the samples except a 265-nm deep UV LED. It is noteworthy that the conversion rates (Fig. 7 (a)) were completely independent of absorption of photoinitiators included (Fig. 7 (b)). On irradiation at 265 nm, BAOBE was the most effective among the photoinitiators used in this study. Effect of 285-nm irradiation on UV curing was in the order, HCPK > BAOBE > DMPA > TPO ~ BAOAE > HMPP. When the films were irradiated at 300 nm, HCPK, DMPA, and TPO were effective. The reaction rates of the films on irradiation below 300 nm were larger than those on irradiation at 365 nm and the cases irradiated by medium pressure mercury

lamp in all cases. The results clearly showed the effectiveness of deep-UV LED lamps on UV curing in air.

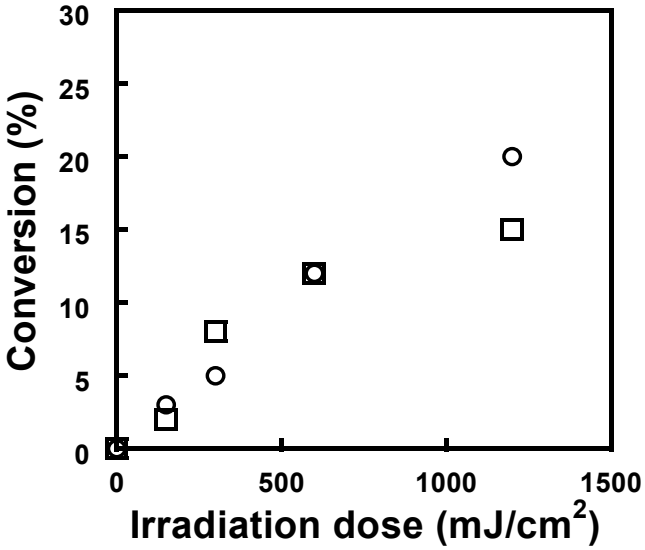

Fig. 6. Conversion of 0.7-μm-thick A-DPH/HCPK (1:0.005, wt/wt) blended films on irradiation at 285 nm. (❍): In air. (□): Laminated. Light intensity: 0.7 mW/cm^2.

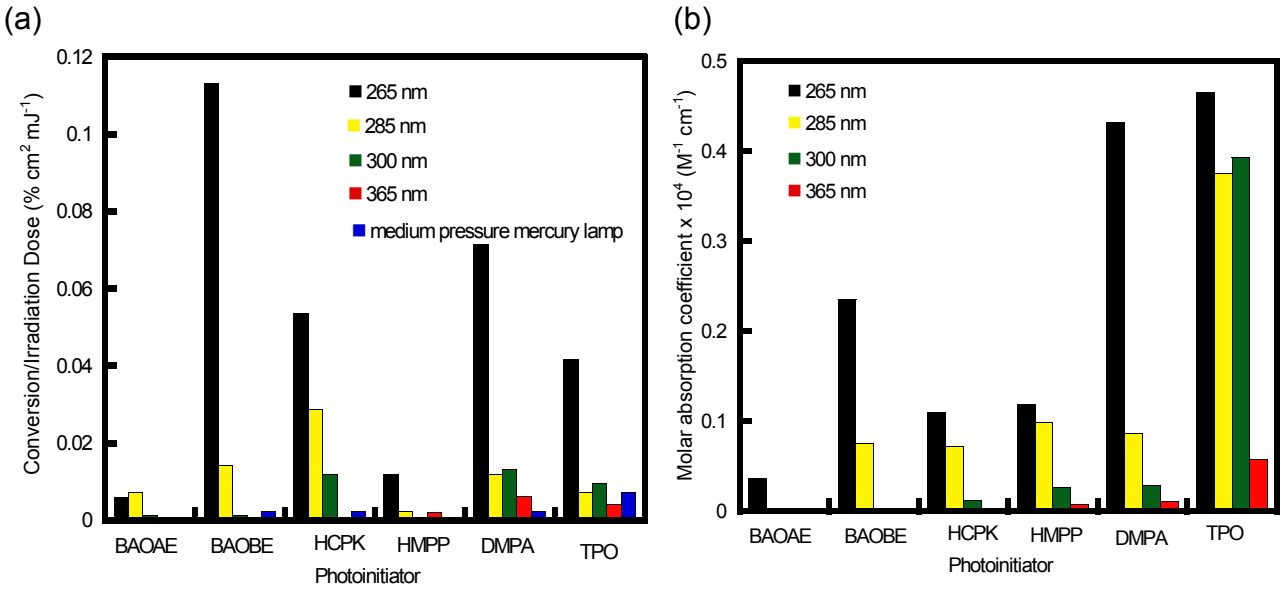

Fig. 7. (a) Conversion rate of 0.7-μm-thick A-DPH/HCPK (1:0.005, wt/wt) blended films in air and (b) molar absorption coefficients of photoinitiators.

In the photoDSC studies, the thickness of the samples ranged from about 200 to 800 μm due to the limitation of the photoDSC instrument used. The light below 300 nm does not completely penetrate the samples in the photoDSC studies.

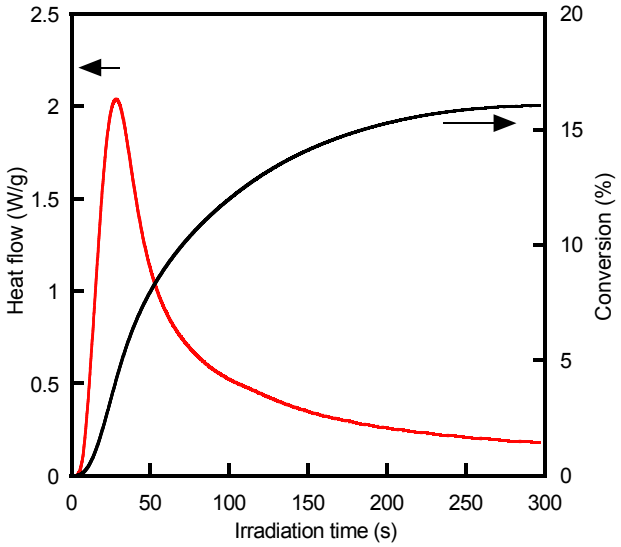

Fig. 8. PhotoDSC curves of 400-μm-thick A-DPH/HCPK (1:0.005, wt/wt) blended film on irradiation at 365 nm in N_2. Red line: heat flow. Black line: conversion. Light intensity: 2.0 mW/cm^2.

PhotoDSC thermograms of 400-μm-thick A-DPH/HCPK (1:0.005, wt/wt) blended film on irradiation at 365 nm in N_2 was shown in Fig. 8. In the case of photoDSC measurements, conversion was not proportional to irradiation dose. The difference is due to high heat formations which accelerate the polymerization reaction. The conversion was calculated using the sum of the heat[13].

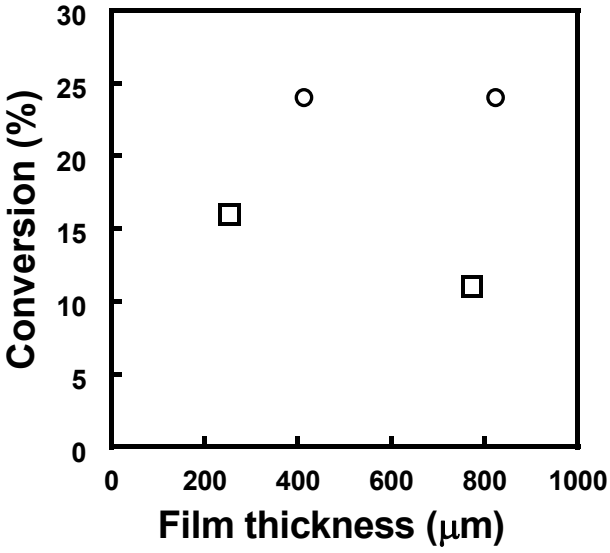

Fig. 9. Conversion of (□) A-DPH/HCPK (1:0.005, wt/wt) and (○) A-TMM-3LMN/HCPK (1:0.005, wt/wt) blended film on irradiation at 365 nm for 10 min in N_2. Light intensity: 2.0 mW/cm^2.

The effects of functionality of acrylates and film thickness on the photocuring behavior were investigated. Figure 9 shows the conversions of A-DPH having six functionalities and A-TMM-3LMN having three functionalities. Conversions of A-TMM-3LMN were higher than those of A-DPH regardless of film thickness. The result is due to higher mobility of propagating radical species in A-TMM-3LMN ascribed to lower crosslinking densities of the crosslinked A-TMM-3LMN instead of A-DPH having six functionalities. The results agreed with the previous report[18].

The effects of atmospheric conditions and the film thickness on the photocuring behavior were discussed. Figure 10 shows conversions of A-DPH/HCPK blended films on irradiation at 285 nm. On irradiation in air, the conversions were about 10% regardless of film thickness. On irradiation in N_2, on the other hand, the conversions increased, then reached maximum value, and decreased with increasing film thickness. The deviation between the value obtained in air and under N_2 shows the degree of oxygen inhibition. We have concluded that oxygen inhibition was effectively suppressed with low film thickness on irradiation at 285 nm. The phenomenon is not observed on irradiation when irradiated at 365 nm.

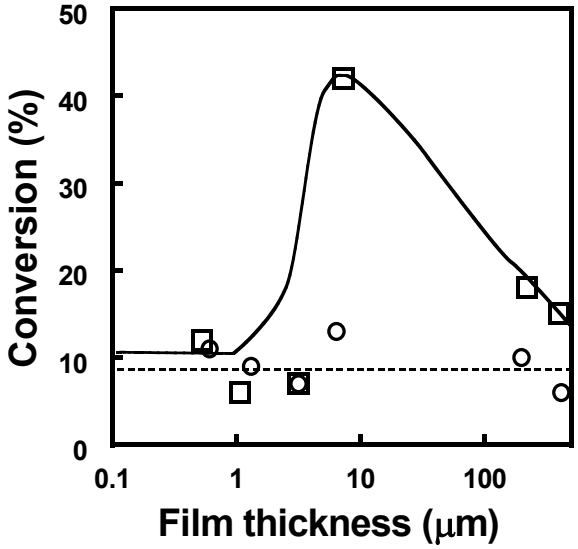

Fig. 10. Conversion of A-DPH/HCPK (1:0.005, wt/wt) blended film on irradiation at 285 nm. (❍) : In air. (□) : Laminated or under N_2. Light intensity: 0.7 mW/cm^2. Irradiation time: 10 min.

The effects of photoradical initiators and irradiation wavelength on the photocuring behavior were investigated using 400-μm-thick films. Figure 11 shows the maximum conversion rate of A-DPH with photoinitiators on irradiation at several wavelengths with (a) and without (b) the effect of oxygen. Maximum conversion rates in Fig. 11 were calculated using the values of maximum heat flows in PhotoDSC measurements. In the experimental conditions, the irradiation lights did not completely penetrate the samples. It is noteworthy that oxygen inhibition is observed for any photoinitiators investigated. Thus, we concluded that irradiation by deep UV LED was effective using BAOBE, HCPK, DMPA, and TPO as photoinitiators and the thickness of the formulation is less than several micrometers.

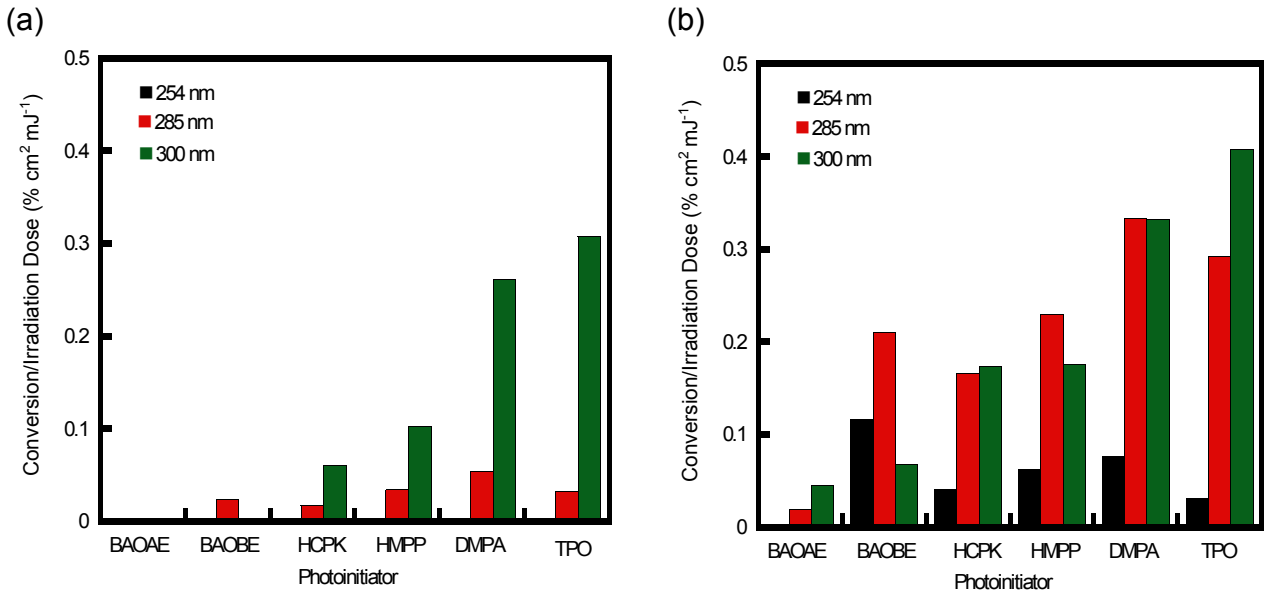

Fig. 11. (a) Maximum conversion rate of 400-μm-thick A-DPH/HCPK (1:0.005, wt/wt) blended films in air (a) and under N_2 (b).

Conclusions

We investigated the formulations of acrylates which were applicable to deep UV LED lamps. The mixtures of acrylate monomers and photoinitiators were placed on silicon wafer or sandwiched between a silicon plate and a CaF_2 plate to obtain sample films. The films were irradiated by deep UV lamps which emit 265, 285, and 300-nm lights. The effect of initiators, irradiation wavelength, and atmosphere on the conversion of the acryl unit was investigated using FT-IR spectroscopy. We found that the photoinitiator *O*-benzoyl 2,3-butanedione monooxime (BAOBE) was the most effective photoinitiator investigated on irradiation at 265 nm. A conventional photoinitiator 1-hydroxy-1-cyclohexyl phenyl ketone (HCPK) was also useful in addition to BAOBE on irradiation at 285 nm. Conventional photoinitiators HCPK, 2,2-dimethoxy-2-phenylacetophenone, and diphenyl(2,4,6-trimethylbenzoyl)phosphine oxide were also effective on irradiation at 300 nm. Irradiation by deep UV LEDs is effective to suppress oxygen inhibition for less than several micrometer-thick films containing the photoinitiators.

References

1. J. P. Fouassier, J. F. Rabek, *Radiation Curing in Polymer Science and Technology*, Elsevier Applied Science, New York (1993).
2. K. C. Anyaogu, A. A. Ermoshkin, D. C. Neckers, A. Mejiritski, O. Grinevich, A. V. Fedorov, *J. Appl. Polym. Sci.*, **105**, 803 (2007).
3. M.-A. Tehfe, F. Dumur, B. Graff, F. Morlet-Savary, J.-P. Fouassier, D. Gigmes, J. Lalevée, *Macromolecules*, **45**, 8639 (2012).
4. P. Xiao, F. Dumur, B. Graff, D. Gigmes, J. P. Fouassier, J. Lalevée, *Macromolecules*, **47**, 601 (2014).
5. J. Zhang, P. Xiao, F. Morlet-Savary, B. Graff, J. P. Fouassier, J. Lalevée, *Polym. Chem.*, **5**, 6019 (2014).

6. P. Xiao, F. Dumur, J. Zhang, B. Graff, D. Gigmes, J. P. Fouassier, J. Lalevée, *Macromol. Chem. Phys.*, **216**, 1782 (2015).
7. X. Dong, W. Shen, P. Hu, Z. Li, R. Liu, X. Liu, *J. Appl. Polym. Sci.*, in press. DOI: 10.1002/app.43239.
8. F. Karasu, C. Croutxe-Barghorn, X. Allonas, L. G. J. Van Der Ven, *J. Polym. Sci. Part A: Polym. Chem.*, **52**, 3597 (2014).
9. Y. Aoyagi, M. Takeuchi, K. Yoshida, M. Kurouchi, T. Araki, Y. Nanishi, H. Sugano, Y. Ahiko, H. Nakamura, *J. Environ. Prot.*, **3**, 695 (2012).
10. S. Sharma, H. Dennis Tolley, P. B. Farnsworth, M. L. Lee, *Anal. Chem.*, **87**, 1381 (2015).
11. J.-y. Bae, Y. H. Kim, H. Y. Kim, Y. B. Kim, J. Jin, B.-S. Bae, *ACS Appl. Mater. Interfaces*, **7**, 1035 (2015).
12. S. I. Hong, T. Kurosaki, M. Okawara, *J. Polym. Sci. Polym. Chem. Ed.*, **12**, 2553 (1974).
13. K. S. Anseth, C. M. Wang, C. N. Bowman, *Macromolecules*, **27**, 650 (1994).
14. H. F. Gruber, *Prog. Polym. Sci.*, **17**, 953 (1992).
15. H. Okamura, M. Kayanoki, K. Takada, H. Nakajiri, K. Muramatsu, M. Yamashita, M. Shirai, *Polym. Adv. Technol.*, **23**, 1151 (2012).
16. P. Baas, H. Cerfontain, *J. Chem. Soc., Perkin Trans.*, **2**, 1653 (1979).
17. J. Ann, *UV+EB Technol.*, (3) 48 (2015).
18. I. V. Khudyakov, J. C. Legg, M. B. Purvis, B. J. Overton, *Ind. Eng. Chem. Res.*, **38**, 3353 (1999).